CHARACTERISTICS OF VORTEX ORGANIZATION IN THE OUTER LAYER OF WALL TURBULENCE

Kenneth T. Christensen and Yanhua Wu
Department of Theoretical and Applied Mechanics,
University of Illinois
Urbana, IL 61801 USA
ktc@uiuc.edu

ABSTRACT

Recent experimental and computational studies support the notion that the outer layer of wall turbulence is populated by hairpin-like vortices which tend to organize themselves into larger-sale coherent groups. The present effort attempts to evaluate the characteristics of this large-scale organization. Wide-field-of-view ($2.5h \times h$) velocity fields are acquired by PIV in the streamwise–wall-normal plane of turbulent channel flow for $744 < \mathrm{Re}_\tau < 2099$ in order to study the imprint of this organization upon multi-point statistics as well as its average characteristics. Comparisons of unconditional and conditional two-point correlations of streamwise velocity indicate that outer-layer vortex organization leaves a definitive imprint upon multi-point statistics, highlighting its statistical significance. Its average streamwise extent, estimated from two-point velocity correlations, is found to increase with Re_τ, even when scaled in outer units. Further, its streamwise extent grows substantially within the log layer. In contrast, the average inclination angle of the packets appears to be independent of Re_τ and relatively insensitive to wall-normal position outside the near-wall region.

INTRODUCTION

There is broad evidence that a vortical structure qualitatively similar to the "horseshoe vortex" proposed by Theodorsen (1952) does exist in canonical smooth-wall turbulence at both low and high Reynolds numbers (Re). At low Re, Smith (1984) reported the existence of hairpin vortices[1] and proposed an organized alignment of these structures in the streamwise direction. This work was later extended to argue that hairpin vortices can actually regenerate from an existing vortex (Smith et al., 1991). Similar organization was noted by Zhou et al. (1997, 1999) who studied the evolution of an initial structure in a direct numerical simulation (DNS) of turbulent channel flow. Given sufficient strength of the initial structure, multiple hairpin-like vortices spawned both upstream and downstream of the initial structure, creating a coherent alignment of vortices termed a *hairpin vortex packet*. The legs of vortices residing in the log layer were commonly observed to extend below $y^+ = 60$, consistent with the near-wall quasi-streamwise vortex observations of Brooke and Hanratty (1993), Schoppa and Hussain (1997) and Heist et al. (2000), among others. Further, the notion of coherent vortex organization provides a structural explanation for both the long streamwise extent of low-speed streaks and the observation of multiple ejections within a single bursting event (Kline et al., 1967; Bogard and Tiederman, 1986; Tardu, 1995).

The structure of the outer region of wall turbulence (defined herein as the log layer and beyond) has certainly not received as much attention as the structure of the near-wall region. However, it has been established that the outer layer is populated by inclined structures that are associated with ejections and sweeps (Brown and Thomas, 1977; Head and Bandyopadhyay, 1981; Bogard and Tiederman, 1986; Tardu, 1995). Head and Bandyopadhyay (1981) observed hairpin-like structures in smoke visualizations of a zero-pressure-gradient turbulent boundary layer at higher Re ($\mathrm{Re}_\theta \leq 17500$). They also noted ramp-like patterns at the outermost edge of the boundary layer and proposed these patterns to be the imprint of groups of hairpin-like vortices inclined away from the wall at a shallow angle. More recently, PIV measurements in a turbulent boundary layer by Adrian et al. (2000) provide strong evidence that hairpin-like structures occur throughout the outer layer and align to create larger-scale *packets*. This outer-layer organization is characterized by a series of hairpin-like vortices aligned in the streamwise direction whose heads form an interface slightly inclined away from the wall and a region of relatively uniform, low-momentum fluid beneath the interface attributable to the collective induction of the vortices. The PIV data permitted visualization of this organization within the interior of the boundary layer, showing that packets occur throughout the outer region in a hierarchy of scales. Finally, Christensen and Adrian (2001) used conditional averaging techniques to show that this organization is a dominant and coherent feature of the flow, while Marusic (2001) determined that the long streamwise tail of the streamwise velocity correlation (ρ_{uu}) in the log layer is attributable to outer-layer vortex organization.

Substantial evidence exists establishing not only the existence of outer-layer vortex organization but also its significance to the overall dynamics of the flow as well. Therefore, the exact statistical impact and the spatial characteristics of this behavior must be understood before it can be accounted for in numerical and physical models of wall turbulence. The present effort attempts to address such issues.

EXPERIMENT

Extensive measurements are made in a turbulent channel flow facility with a development length of $252h$ (where $h = 25\,\mathrm{mm}$ is the half-height of the channel) and an aspect ratio of 12:1. The working fluid of the tunnel is air and the flow is conditioned by a series of screens, honeycomb, and a

[1]The term "hairpin vortex" is used here to describe both symmetric and asymmetric hairpin-, lambda- and arch-like structures.

contraction, producing a near-uniform flow with minimal disturbance at the entrance of the channel. Static pressure taps are mounted along the length of the channel allowing direct documentation of the wall shear stress, τ_w. Glass windows in the test section provide optical access from all directions. Fluid properties are determined from measurements of the atmospheric pressure and fluid temperature using an ideal gas relation in concert with Sutherland's correlation for viscosity. This information is then used to determine the friction velocity, $u_* = (\tau_w/\rho)^{1/2}$, and the viscous length scale, $y_* = \nu/u_*$.

Particle-image velocimetry (PIV) is used to measure two-dimensional velocity (u, v) fields in the streamwise–wall-normal $(x-y)$ plane along the channel's spanwise centerline at three distinct Reynolds numbers: $\mathrm{Re}_\tau \equiv u_* h/\nu = 744, 1425$ and 2099. The field of view is $2.5h \times h$ $(x \times y)$, permitting extensive study of large-scale features in the streamwise direction. The air flow is seeded with nominally $1\,\mu$m olive oil droplets and the field of view is illuminated with lightsheets formed from a pair of New Wave Research Gemini Nd:YAG lasers. Each laser pulse has a temporal width of 5 ns and approximately 80 mJ of energy. The nominal thickness of the lightsheets in the test section is approximately $150\,\mu$m. The scattered light from the seed particles is captured by a 1280×1024 pixel TSI PIVCAM 13-8 12-bit CCD camera with frame-straddle capabilities and a 105-mm focal length lens is used to image the particles with an f-number of 8. Two distinct images are acquired per vector field with a fixed time delay, facilitating two-frame cross-correlation analysis of the images.

The pairs of PIV images are interrogated using the *PIV Sleuth* software package (Christensen et al., 2000). The images are subdivided into square interrogation windows and a larger second window is selected to minimize bias errors associated with loss of image pairs. The images are analyzed with 50% overlap to satisfy Nyquist's criterion and the second window is offset in the mean flow direction by the bulk displacement of the flow. The image ensembles are interrogated using first interrogation windows of size 16×16 pixels at all three Re_τ, yielding a vector grid spacing of $0.015h$, or $11.3y_*$, $21.6y_*$ and $31.8y_*$ at $\mathrm{Re}_\tau = 744$, 1425 and 2099, respectively. The instantaneous vector fields in each ensemble are then validated using objective statistical methods to remove any erroneous velocity vectors. Holes are filled either with alternative velocity choices determined *a priori* during interrogation or interpolated in regions where at least 50% of neighbors are present. On average, over 99% of the velocity vectors in a given field are found to be valid *prior* to replacement and interpolation. Finally, each vector field is low-pass filtered with a narrow Gaussian filter to remove any noise associated with frequencies larger than the sampling frequency of the interrogation. Two-thousand statistically-independent velocity fields are acquired at each Re_τ, facilitating the calculation of accurate statistics. Table 1 summarizes the relevant flow parameters for all experimental conditions studied.

Table 1: Summary of flow parameters for all experiments.

Re_τ	τ_w (Pa)	u_* (m/s)	y_* (μm)	Δx^+	Δy^+	Δz^+
744	0.29	0.53	23.6	11.3	11.3	6.4
1425	1.09	1.04	17.6	21.6	21.6	8.5
2099	2.38	1.54	11.9	31.8	31.8	12.6

RESULTS

Instantaneous structure

Figure 1 shows typical instantaneous PIV velocity fields in the streamwise–wall-normal plane of the channel at (a) $\mathrm{Re}_\tau = 744$, (b) $\mathrm{Re}_\tau = 1425$, and (c) $\mathrm{Re}_\tau = 2099$. A constant advection velocity is removed from each field, revealing those vortex cores advecting at this speed. These spanwise vortex cores have clockwise rotation (negative spanwise vorticity, ω_z) and are believed to be the heads of hairpin-like vortices advecting as a larger-scale coherent entity in the streamwise direction (Zhou et al., 1999; Adrian et al., 2000; Christensen and Adrian, 2001). A lifting of low-speed fluid away from the wall (referred to as a Q_2 event in the nomenclature introduced by Wallace et al. (1972)) just under and upstream of each vortex is consistent with the hairpin vortex signature introduced by Adrian et al. (2000). Vortex packets are visible at all three Re_τ, with the outer edge of each packet roughly defined by the dashed lines superimposed on the velocity fields. Two packets are visible at $\mathrm{Re}_\tau = 744$, with the upstream packet having a smaller inclination angle (10°) and shorter streamwise extent than the downstream one (17°). A single vortex packet is observable in the $\mathrm{Re}_\tau = 1425$ example. This packet extends over nearly the entire streamwise field of view, it has an inclination angle of roughly 12°, and the downstream-most vortex in the packet extends to nearly $0.6h$ in the wall-normal direction. Finally, at $\mathrm{Re}_\tau = 2099$, several spanwise vortex cores are aligned in the streamwise direction, yielding a packet that extends nearly $2.5h$ in x with an inclination angle of 13°.

All of the packet examples noted in Figure 1 are also marked by elongated regions of low momentum fluid beneath the inclined interface demarcated by the spanwise vortex cores. These low-momentum regions are attributable to the collective induction of the vortices within a packet and can be quite long in the streamwise direction. Additionally, these examples indicate that vortices within a given packet can extend well beyond the log layer and the streamwise spacing of vortices within a packet can vary, with vortices closer to the wall seemingly spaced closer together than vortices further away from the wall (Figure 1(c), for example). The character of these instantaneous realizations is entirely consistent with the results of Zhou et al. (1997, 1999) and Adrian et al. (2000), indicating that vortex organization is a common feature in the outer region of wall-bounded turbulent flows.

It is important to note that the examples of outer-layer vortex organization presented in Figure 1 are not isolated occurrences. Rather, similar patterns are noted in a vast majority of the statistically-independent instantaneous velocity realizations at all three Re_τ. This observation indicates that outer-layer vortex organization is a robust and dominant feature of wall turbulence. However, the spatial characteristics of this outer-layer organization do vary slightly from packet to packet. In particular, the streamwise length of the packets can vary from realization to realization, as can the inclination angle.

Two-point velocity correlations

Two-point spatial velocity correlation coefficients of the

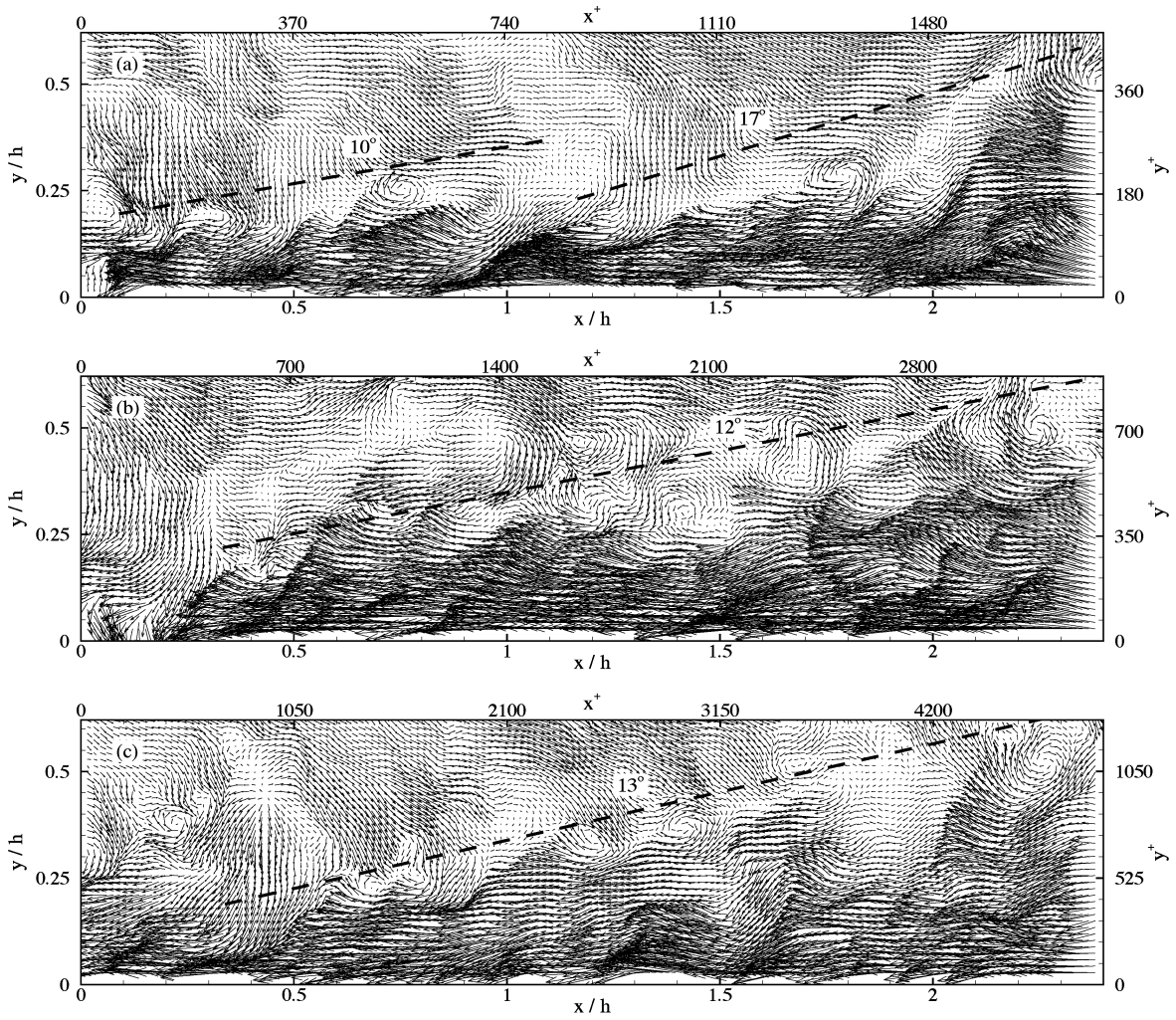

Figure 1: Instantaneous velocity realizations in the streamwise–wall-normal $(x-y)$ plane of turbulent channel flow with a constant advection velocity removed. (a) $\mathrm{Re}_\tau = 744$; (b) $\mathrm{Re}_\tau = 1425$; (c) $\mathrm{Re}_\tau = 2099$. The flow is from left to right.

form

$$\rho_{ij}(r_x, y; y_{ref}) = \frac{\langle u_i'(x, y_{ref}, t) u_j'(x + r_x, y, t)\rangle}{\sigma_i(y_{\mathrm{ref}})\sigma_j(y)}, \qquad (1)$$

are computed from the velocity-field ensembles at each Re_τ to assess the statistical impact of outer-layer vortex organization. In Eqn. (1), r_x represents the spatial separation in the streamwise direction (since it is statistically homogeneous) and u_i' and σ_i denote the fluctuation and root-mean-square of the i^{th} velocity component, respectively[2]. For brevity, the discussion herein will be limited to the impact of outer-layer vortex organization on the two-point correlation of streamwise velocity, ρ_{uu}.

Figure 2(a–c) presents ρ_{uu} (ρ_{11}) at $y_{\mathrm{ref}} = 0.1h$ for $\mathrm{Re}_\tau = 744$, 1425, and 2099, respectively. Clearly, ρ_{uu} is quite elongated in the streamwise direction at all three Re_τ. For a correlation coefficient level of 0.5, for example, ρ_{uu} is on the order of h in all cases. This spatial extent is certainly consistent with the streamwise length of the low-momentum regions created by vortex packets observed in instantaneous velocity realizations (Figure 1). Additionally, this length appears to be Reynolds-number dependent (even when scaled by h), with packets at larger Re_τ having slightly longer streamwise extents. In addition, ρ_{uu} is inclined away from the wall at a shallow angle which is certainly similar to the inclination of the instantaneous vortex packets noted in Figure 1.

These consistencies between ρ_{uu} and the large-scale spatial characteristics of instantaneous vortex packets *indirectly* support the notion that outer-layer vortex organization leaves a definitive imprint upon ρ_{uu}. This consistency may be expected since vortex packets occur in a vast majority of the statistically-independent velocity realizations at all three Re_τ. To further quantify the "occurrence rate" of vortex packets in the statistically-independent instantaneous velocity fields, the ensembles of velocity fields at each Re_τ are separated into two categories: fields that contain outer-layer vortex organization and fields that do not. This separation is achieved manually by simply visualizing each instantaneous velocity field in a Galilean frame. Those fields which exhibit clear organization and inclination of spanwise vortex cores and long regions

[2]The spanwise direction is neglected in this representation since the PIV data resides in the streamwise–wall-normal plane.

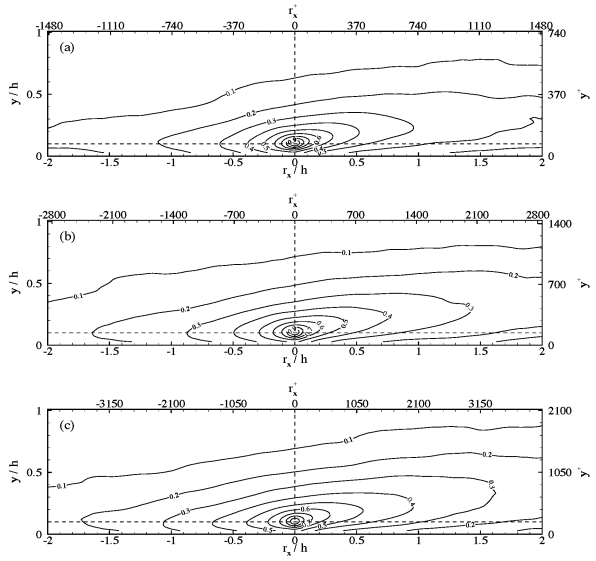

Figure 2: Two-point correlation coefficients of the streamwise velocity fluctuations, ρ_{uu}, for $y_{\text{ref}} = 0.1h$. (a) $\text{Re}_\tau = 744$; (b) $\text{Re}_\tau = 1425$; (c) $\text{Re}_\tau = 2099$.

of relatively uniform momentum deficit (like the fields presented in Figure 1) are deemed to contain vortex packets. Table 2 summarizes the number of statistically-independent velocity realizations containing outer-layer organizations at each Re_τ. *At least 65% of the realizations contain definitive outer-layer vortex organization at all three Re_τ meaning that one should expect this organization to contribute significantly to the overall statistics of the flow.* It is crucial to note that the velocity fields in each Re_τ ensemble are *statistically independent*, meaning these ensembles represent a *random* sampling of the overall flow behavior.

Conditional two-point velocity correlations

One can further confirm the connection between the spatial character of ρ_{uu} and the characteristics of large-scale vortex organization by considering the relative contributions to ρ_{uu} from velocity fields that exhibit clear outer-layer vortex organization versus those that do not. One can express this simple "decomposition" as

$$\rho_{uu}(r_x, y; y_{ref}) = \hat{\rho}^P_{uu}(r_x, y; y_{ref}) + \hat{\rho}^{NP}_{uu}(r_x, y; y_{ref}), \quad (2)$$

where ρ_{uu} represents the unconditional correlation coefficient of streamwise velocity, $\hat{\rho}^P_{uu}$ embodies the contributions to ρ_{uu} from the velocity fields that contain outer-layer vortex organization and $\hat{\rho}^{NP}_{uu}$ represents the contribution from the velocity fields that do not contain vortex packets. Figure 3 presents $\hat{\rho}^P_{uu}$ ((a–c)) and $\hat{\rho}^{NP}_{uu}$ ((d–f)) at $\text{Re}_\tau = 744, 1425$ and 2099, respectively. All three Re_τ examples confirm that outer-layer vortex organization contributes significantly to the overall characteristics of ρ_{uu}, particularly in the region $|r_x| \leq h$ where one would expect its influence to be strongest. In this region, nearly 75% of ρ_{uu} is associated with the velocity realizations containing vortex packets, indicating that the long streamwise extent and shallow inclination of ρ_{uu} are indeed a direct consequence of outer-layer vortex organization. In contrast, the velocity fields devoid of vortex organization contribute very little to ρ_{uu} and have virtually no inclination away from the wall except near $r_x = 0$. One might argue that the strong contribution from the velocity fields containing vortex organization is simply attributable to the fact that many more velocity fields contain vortex packets than do not. This is indeed the case, but one must realize that the velocity-field ensembles presented herein represent a *random* samplings of the flow, meaning that packets *naturally* occur a majority of the time in this flow and hence they *naturally* contribute significantly to the overall character of the flow.

Table 2: Number of realizations at each Re_τ containing outer-layer vortex organization.

Re_τ	Total No. Realizations	No. Realizations w/ Packets	No. Realizations w/o Packets
744	2000	1526 (76.3%)	474 (23.7%)
1425	2000	1306 (65.3%)	694 (34.7%)
2099	2000	1386 (69.3%)	614 (30.7%)

Given the significant imprint that outer-layer vortex organization leaves upon ρ_{uu}, the average vortex-packet length can be estimated from the average streamwise extent of ρ_{uu}. In addition, the average inclination angle of outer-layer vortex organization can be assessed by considering the inclination angle of ρ_{uu}. Although such estimates are not exact measures of the average length and inclination angle of the packets, they do provide a means of bounding these quantities and studying their trends with Re_τ and y.

Streamwise extent of ρ_{uu}

The average streamwise extent of ρ_{uu} can be assessed by considering one-dimensional slices through the two-dimensional correlation coefficients for $y = y_{\text{ref}}$. However, since the long streamwise tail of ρ_{uu} is not captured in this data, computation of a true integral length scale is not possible. In addition, noise due to statistical sampling errors at the largest spatial separations render even estimates of the integral length scale inaccurate. Therefore, in order to avoid these issues, we choose to define the average streamwise extent of ρ_{uu} by thresholding the one-dimensional streamwise correlation coefficients at 50% correlation. Based upon thresholding, we define the average streamwise length scale of ρ_{uu} as

$$L_x = 2r_x|_{\rho=0.5}. \quad (3)$$

Figure 4(a,b) illustrates the average streamwise extent of ρ_{uu}, L_x, as a function of y plotted in inner and outer units, respectively. As Re_τ increases, L_x increases in both inner and outer scalings. This Re_τ-trend indicates that the large-scale structures of the flow, presumably the vortex packets, grow in streamwise length with Re_τ. This growth may be attributable to the average number of vortices per packet increasing with Re_τ and/or an increase in the average streamwise spacing of consecutive vortices within a packet with Re_τ.

For fixed Re_τ, the streamwise extent of ρ_{uu} grows substantially with y in the log layer ($y^+ > 100$, $y < 0.2 - 0.3h$). This behavior may indicate that packet development occurs predominantly in the log region. Outside the log layer, L_x remains roughly constant until approximately $y = 0.6h$, beyond which it decreases as the centerline of the channel is approached. These trends may support the idea that the

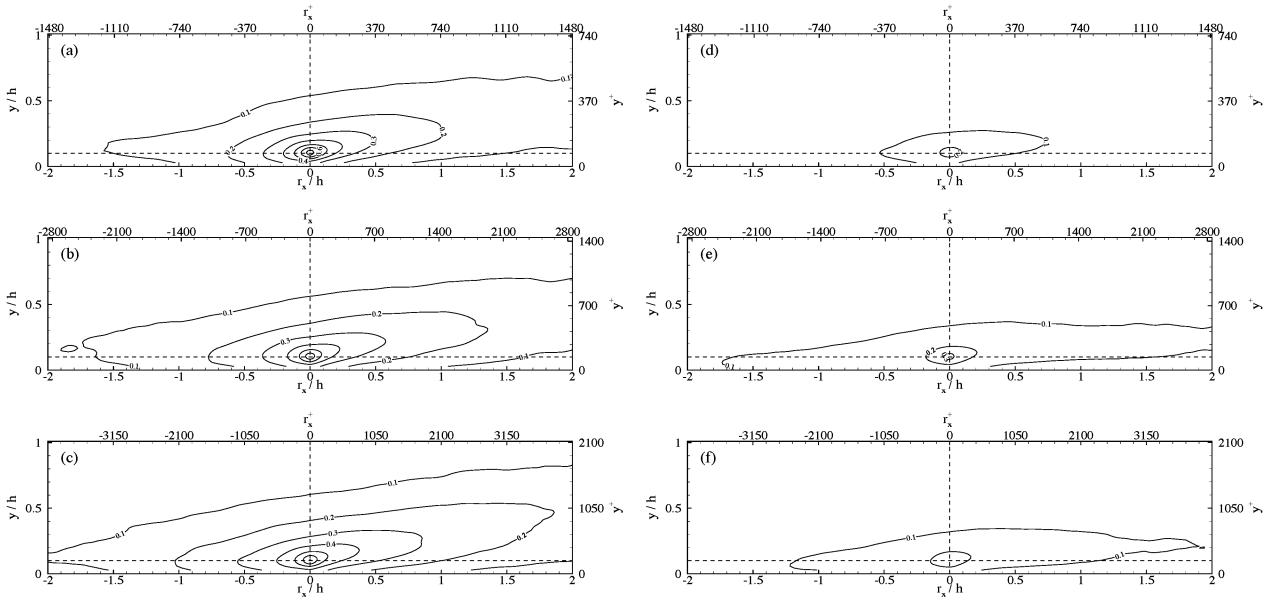

Figure 3: Conditional two-point correlation coefficients of the streamwise velocity fluctuations for $y_{\mathrm{ref}} = 0.1h$. (a)–(c): Computed from velocity fields containing packets, $\hat{\rho}_{uu}^{P}$, at $\mathrm{Re}_\tau = 744, 1425$ and 2099, respectively; (d)–(f): Computed from velocity fields containing no packets, $\hat{\rho}_{uu}^{NP}$, at $\mathrm{Re}_\tau = 744, 1425$ and 2099, respectively.

building-blocks of vortex packets are born within the near-wall and log layers where the mean shear is strongest, and simply grow and mature beyond the log layer. For $y > 0.6h$, vortex organization appears to break down, with the average streamwise extent steadily decreasing toward the centerline of the channel. This behavior may be due to strong interactions with the flow on the opposing wall beyond $y = 0.6h$.

Average inclination angle

The inclination angle of ρ_{uu}, which represents an estimate of the average inclination angle of outer-layer vortex organization, is assessed by extracting the line of maximum correlation for each y_{ref}. If one roughly models the correlation contours in Figure 2 as ellipses, then the line of maximum correlation would be coincident with the major axis of the ellipse. This line is determined using least-squares methods from a series of points extracted for five different contour levels: 0.9, 0.8, 0.7, 0.6 and 0.5. The point that is farthest away from the self-correlation peak ($r_x = 0$, $y = y_{\mathrm{ref}}$) is extracted for each contour level. Since these points presumably lie upon the line of maximum correlation, a linear fit of these points is performed and the inclination angle of this line relative to the wall is determined. This analysis is repeated for each contour map corresponding to a different y_{ref} at all three Re_τ, yielding estimates of the inclination angle as a function of both y and Re_τ.

The inclination angle of ρ_{uu}, θ, as a function of y for all three Re_τ is presented in Figure 5. A clear Reynolds-number trend is not evident, and the average inclination angle appears relatively insensitive to y, except very close to the wall. Beyond the near-wall region the average inclination angle is roughly constant at approximately 11°. There is some scatter in θ, owing to the extreme sensitivity of the linear fit to small inaccuracies in determining the points of maximum correlation. Nevertheless, the average values of θ presented herein are certainly consistent with the angles noted in the instantaneous velocity realizations in Figure 1 and those reported in the literature (Zhou et al., 1999; Christensen and Adrian, 2001). Note that θ is only presented between $0 < y < 0.6h$ because the correlation contours quickly flatten to zero inclination beyond this point. This transition point is consistent with the y-location where the streamwise extent of ρ_{uu} begins to decrease, and further supports the notion that vortex organization may break down beyond $y = 0.6h$ in turbulent channel flow.

SUMMARY

Outer-layer vortex organization is found to occur quite often in statistically-independent instantaneous velocity fields acquired in turbulent channel flow and, as a consequence, contributes significantly to the spatial statistics of the flow. In particular, outer-layer vortex organization accounts for nearly 75% of ρ_{uu} for $|r_x| < h$, and is responsible for its long streamwise extent and shallow inclination angle. For fixed y, the average streamwise extent of vortex organization is found to increase with Re_τ. Further, for fixed Re_τ, its average length increases profoundly until the outer edge of the log layer, beyond which it becomes roughly constant until $y = 0.6h$. In contrast, the average inclination angle of this organization is roughly 11° and appears relatively insensitive to both Re_τ and y.

ACKNOWLEDGEMENTS

The experiments presented herein were performed with equipment on loan from Dr. W. Lai at TSI, Inc. and the analysis portion of this effort was financially supported by the University of Illinois and Oak Ridge Associated Universities.

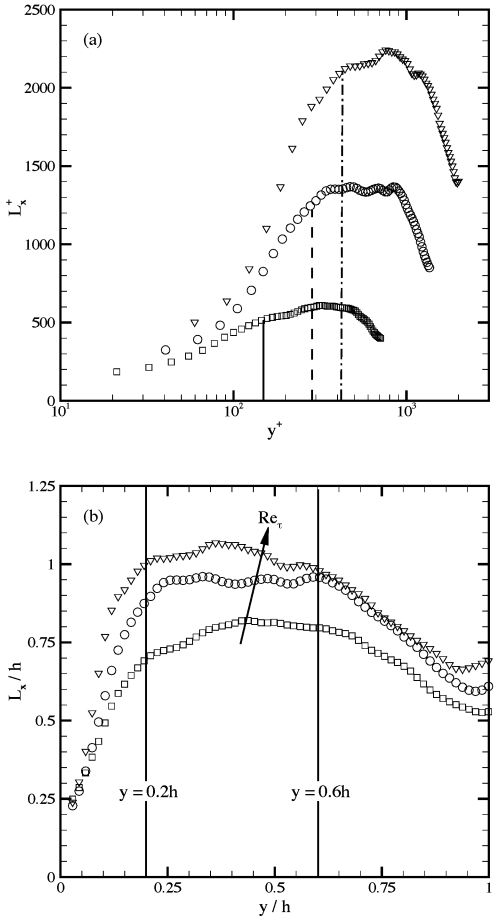

Figure 4: Average streamwise extent of ρ_{uu}, L_x, in (a) inner units and (b) outer units. □: $\mathrm{Re}_\tau = 744$; ◯: $\mathrm{Re}_\tau = 1425$; ∇: $\mathrm{Re}_\tau = 2099$. Lines in (a) demarcate $y = 0.2h$ (the outer edge of the log layer) for each Reynolds number. Every other data point shown for clarity.

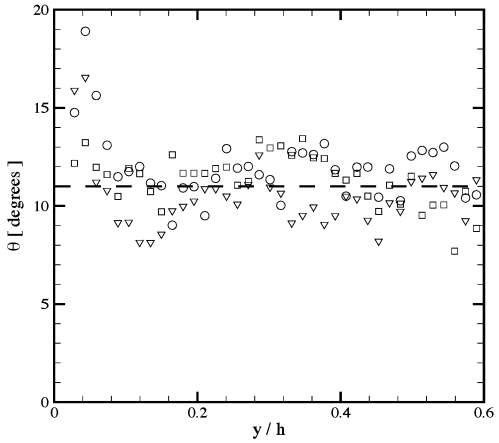

Figure 5: Average inclination angle of ρ_{uu} as a function of wall-normal position. □: $\mathrm{Re}_\tau = 744$; ◯: $\mathrm{Re}_\tau = 1425$; ∇: $\mathrm{Re}_\tau = 2099$. Dashed line denotes $\theta = 11°$.

REFERENCES

R. J. Adrian, C. D. Meinhart, and C. D. Tomkins. Vortex organization in the outer region of the turbulent boundary layer. *J. Fluid Mech.*, 422:1–54, 2000.

D. G. Bogard and W. G. Tiederman. Burst detection with single-point velocity measurements. *J. Fluid Mech.*, 162: 389–413, 1986.

J. W. Brooke and T. J. Hanratty. Origin of turbulence-producing eddies in a channel flow. *Phys. Fluids*, 5(4): 1011–1022, 1993.

G. R. Brown and A. S. W. Thomas. Large structure in a turbulent boundary layer. *Phys. Fluids*, 20:S243–251, 1977.

K. T. Christensen and R. J. Adrian. Statistical evidence of hairpin vortex packets in wall turbulence. *J. Fluid Mech.*, 431:433–443, 2001.

K. T. Christensen, S. M. Soloff, and R. J. Adrian. PIV Sleuth: Integrated particle-image velocimetry (PIV) interrogation/validation software. Technical Report 943, Department of Theoretical and Applied Mechanics, University of Illinois at Urbana-Champaign, 2000.

M. R. Head and P. Bandyopadhyay. New aspects of turbulent boundary-layer structure. *J. Fluid Mech.*, 107:297–338, 1981.

D. K. Heist, T. J. Hanratty, and Y. Na. Observations of the formation of streamwise vortices from arch vortices. *Phys. Fluids*, 12(11):2965–2975, 2000.

S. J. Kline, W. C. Reynolds, F. A. Schraub, and P. W. Runstadler. The structure of turbulent boundary layers. *J. Fluid Mech.*, 30:741–773, 1967.

I. Marusic. On the role of large-scale structures in wall turbulence. *Phys. Fluids*, 13(3):735–743, 2001.

W. Schoppa and F. Hussain. Genesis and dynamics of coherent structures in near-wall turbulence: A new look. In R. L. Panton, editor, *Self-Sustaining Mechanisms of Wall Turbulence*, chapter 16, pages 385–422. Computational Mechanics Publications, 1997.

C. R. Smith. A synthesized model of the near-wall behavior in turbulent boundary layers. In *Proceedings of the* 8^{th} *Symposium on Turbulence*, pages 299–325, Univ. Missouri-Rolla, Rolla, Missouri, 1984.

C. R. Smith, J. D. A. Walker, A. H. Haidari, and U. Sobrun. On the dynamics of near-wall turbulence. *Philosophical Transactions of the Royal Society of London A*, 336:131–175, 1991.

S. Tardu. Characteristics of single and clusters of bursting events in the inner layer, Part 1: VITA events. *Exp. Fluids*, 20:112–124, 1995.

T. Theodorsen. Mechanism of turbulence. In *Proceedings of the 2nd Midwestern Conference on Fluid Mechanics*, pages 1–19, Ohio State University, Columbus, Ohio, 1952.

J. M. Wallace, H. Eckelmann, and R. S. Brodkey. The wall region in turbulent shear flow. *J. Fluid Mech.*, 54:39–48, 1972.

J. Zhou, R. J. Adrian, S. Balachandar, and T. M. Kendall. Mechanisms for generating coherent packets of hairpin vortices in channel flow. *J. Fluid Mech.*, 387:353–396, 1999.

J. Zhou, C. D. Meinhart, S. Balachandar, and R. J. Adrian. Formation of coherent hairpin packets in wall turbulence. In R. L. Panton, editor, *Self-Sustaining Mechanisms of Wall Turbulence*, pages 109–134. Computational Mechanics Publications, Southampton, UK, 1997.